Available online at www.sciencedirect.com
SCIENCE DIRECT®
Journal of Pharmaceutical and Biomedical Analysis
34 (2004) 1079–1090
JOURNAL OF PHARMACEUTICAL AND BIOMEDICAL ANALYSIS
www.elsevier.com/locate/jpba

Identification of BVT.2938 metabolites by LC/MS and LC/MS/MS after in vitro incubations with liver microsomes and hepatocytes

Per Olof Edlund*, Pawel Baranczewski

Preclinical R&D, Biovitrum AB, Lindhagensgatan 133, SE-112 76 Stockholm, Sweden

Received 3 July 2003; received in revised form 12 December 2003; accepted 14 December 2003

Abstract

The metabolism of the 5HT2c agonist BVT.2938, 1-(3-{2-[(2-ethoxy-3-pyridinyl)oxy]ethoxy}-2-pyrazinyl)-2(*R*)-methylpiperazine, was studied in vitro by incubation with rat, monkey and human liver microsomes as well as cryopreserved hepatocytes, followed by liquid chromatography/mass spectrometry (LC/MS) and LC/MS/MS analysis on a quadrupole-time of flight mass spectrometer for structural elucidation. Deuterium exchange on column was used to differentiate between hydroxylation and N-oxidation. Liver microsomes were incubated in two different buffer systems with optimum conditions for cytochrome P450 activity or UDP-glucuronosyltransferase activity. The major phase I metabolites of BVT.2938 originated from *O*-deethylation of the pyridine ring, *O*-dealkylation of the ethylene bridge, pyrazine ring hydroxylation, hydroxylation of pyridine ring and piperazine ring *N*-hydroxylation. When a hydrogen carbonate buffer system was supplemented with UDPGA, the piperazine carbamoyl-glucuronide from the parent compound was identified together with several glucuronides of the phase I metabolites. The metabolite pattern in hepatocytes was similar to microsomes except that the sulphate at the N-position of the piperazine ring of BVT.2938 was identified, while the carbamoyl-glucuronide was missing. Excellent correlation was obtained between radioactivity detection and the chemiluminescent nitrogen detector when the nitrogen content of the analytes was taken into account.
© 2003 Elsevier B.V. All rights reserved.

Keywords: Drug metabolism; Accurate mass; Deuterium exchange; O-18 labelling; *ipso*-Substitution; Chemiluminescent nitrogen detector; Nitrogen specific detection

1. Introduction

The 5HT2c agonist BVT.2938, 1-(3-{2-[(2-ethoxy-3-pyridinyl)oxy]ethoxy}-2-pyrazinyl)-2(*R*)-methylpiperazine is currently being investigated for its preclinical properties for the treatment of obesity. The primary role of early preclinical investigations is to compare the routes of metabolism between different species prior to toxicological studies and to determine the rate of metabolism by enzyme kinetics to predict the clearance in vivo. Thus it is important to generate metabolites from in vitro experiments that as closely as possible reflect the metabolism in vivo. The aim of the present work was to determine the routes of metabolism of BVT.2938 with the aid of different in vitro systems and different incubation conditions

* Corresponding author. Tel.: +46-8-6973-044; fax: +46-8-6973-295.
E-mail address: per-olof.edlund@biovitrum.com (P.O. Edlund).

0731-7085/$ – see front matter © 2003 Elsevier B.V. All rights reserved.
doi:10.1016/j.jpba.2003.12.010

to generate both phase I and phase II metabolites, and to demonstrate the utility of accurate mass determination of product-ions combined with deuterium exchange experiments for structural analysis. The metabolite pattern from incubations with microsomes at different conditions was compared with cryopreserved hepatocyte incubations in the present work. Accurate mass determination of product ions was useful to differentiate between possible fragmentation pathways after collision induced dissociation (CID). Deuterium exchange experiments are used routinely in many laboratories [1–3] and have proved to be very useful to differentiate between hydroxylation and *N*-oxidation. There has been a renewed interest in the chemiluminescent nitrogen detector (CLND) for quantification of drug candidates [4] and drug metabolites [5] at an early stage in drug research when no reference compounds are available for calibration. The utility of CLND for quantification of BVT.2938 metabolites in microsomal incubations was included in the present work since many metabolites with different nitrogen content were formed and radio labelled compound was available as a reference.

2. Materials and methods

2.1. Chemicals

BVT.2938 and BVT.1545, (2-[(2-ethoxypyridin-3-yl)oxy]ethanol) were synthesized at the Department of Medicinal Chemistry, Biovitrum AB and the [^{14}C]-BVT.2938 was labelled at one of the carbon atoms in the ethylene bridge between the pyrazine and pyridine rings. Acetonitrile (HPLC grade) was obtained from Lab-Scan analytical Sciences (Dublin, Ireland) and deuterium oxide was bought from Cambridge Isotope Laboratories (Andover, MA, USA). $^{18}O_2$ gas was obtained from Larodan Fine Chemicals (Malmö, Sweden). Trifluoroacetic acid (TFA) and NADPH were from Merck (Darmstadt, Germany). Methanol of HPLC grade was from Fluka (Stenheim, Germany). Quaternary amines were obtained from Sigma (St. Louis, MO, USA). The human (pool of 16), male Cynomolgus monkey (pool of six) and male Sprague Dawley rat (pool of 203) liver microsomes were bought from XenoTech LLC (Lenexa, KS, USA). The cryopreserved hepatoctyes: human, male Cynomolgus monkey and male Sprague Dawley rat were bought from In Vitro Technologies Inc. (Baltimore, MA, USA).

2.2. Incubation conditions

The incubations for determination of BVT.2938 metabolites were performed at 37 °C with 1 μg/μl of microsomal protein and 1 mM NADPH in a total volume of 1 ml of 100 mM KPO_4 buffer, pH 7.4. BVT.2938 was dissolved in DMSO and added directly to the incubation to a final concentration of 10 μM. The final concentration of DMSO was under 0.2%. The same amount of DMSO was added to control incubations without BVT.2938. The incubations were started by addition of NADPH and terminated after 1 h with one volume of ice-cold acetonitrile. Precipitated proteins were removed by centrifugation at 3500 rpm for 15 min at 4 °C. Samples for analysis by nitrogen specific detection were terminated with three volumes of cold methanol instead of acetonitrile. For incubation with $^{18}O_2$ gas, rat liver microsomes were suspended in phosphate buffer in a 1 ml Reactivial (Pierce, Rockford, Ill, USA) sealed with a silicon membrane and $^{18}O_2$ was introduced with a syringe needle through the membrane into the suspension. The gas that bubbled through the suspension was diverted to the atmosphere through a second syringe needle during 10 min. The syringe needles were removed and the BVT.2938 solution and NADPH solutions were injected through the membrane for incubation as described above.

For generation of BVT.2938 carbamoyl-glucuronide the samples were incubated during 2 h at 37 °C, with 10 μM BVT.2938, 2 μg/μl of microsomal proteins, alamethicine (50 μg per incubation) and UDPGA at a final concentration of 1 mM. The incubations were performed in hydrogen carbonate buffer, pH 7.4 under 5% CO_2/95% O_2 atmosphere. In order to activate both cytochrome P450 and glucuronosyltransferases (UGTs) simultaneously, the incubations were also supplemented with 1 mM NADPH. The incubations were terminated with 1 ml of ice-cold acetonitrile. Precipitated proteins were removed by centrifugation at 3500 rpm for 15 min at 4 °C.

The cryopreserved hepatocytes were thawed and washed in Williams E Medium (Gibco Ltd., UK). After centrifugation at 50 × *g* over 5 min, at 20 °C, the cells were re-suspended and the viability and cell density were measured by trypan blue exclusion. The viabilities of thawed human, monkey and rat hepatocytes were 98, 58 and 70%, respectively. The cells were diluted in Williams E medium to 2×10^6 cells/ml, and the cell suspensions were incubated for up to 4 h with BVT.2938 at the final concentration of 20 μM. The incubations were terminated with one volume of ice-cold acetonitrile. Precipitated proteins were removed by centrifugation at 3500 rpm for 15 min at 4 °C. The acetonitrile used to terminate of the incubations was evaporated under nitrogen and the samples were filtered through 0.45 μm micro-spin cellulose filters from Alltech Assoc. Inc. (IL, USA).

2.3. Liquid chromatography/mass spectrometry

The samples (25–90 μl) were injected by an auto sampler onto a small molecule trap column (1 mm × 10 mm) from Michrome Bioresources Inc. (Auburn, CA, USA) in a flow of 0.02% TFA in water at 0.2 ml/min during 2.6 min pumped by a Shimadzu pump model LC10AD (Kyoto, Japan). The trap column was connected to a six-port valve on a Waters CapLC system (Milford, MA, USA). The analytes were separated on 5 μm Luna C18 particles (1 mm × 150 mm) from Phenomenex (Torrance, CA, USA) with an acetonitrile gradient from the CapLC system after switching of the six-port valve. The gradient consisted of buffer A: 2% acetonitrile and 0.02% TFA in water, buffer B: 0.02% TFA in acetonitrile. The gradient schedule was 0–60% B for 25 min at 0.04 ml/min. The column was re-equilibrated with 0% B during 5 min prior to the next injection. Electrospray mass spectra were recorded in the positive ion-mode on a Q-Tof II mass spectrometer from Micromass (Manchester, UK). Mass spectra were recorded with a cone voltage ramp between 15 and 40 V with an accumulation time of 2 s. Product-ion spectra were recorded at three different collision energies (10, 20 and 40 eV) with an accumulation time of 1 s for each energy and Ar as collision gas. For accurate mass measurements the mass spectrometer was tuned to give a resolution of about 7000 (50% valley) and calibrated with propylamine plus a series of quaternary amines from tetramethyl ammonium to tetraoctyl ammonium. During accurate mass measurements of product-ions from protonated BVT.2938, the precursor ion was first used for lock-mass correction at low collision energy (10–20 eV) and then the product-ion at *m/z* 221.1402 ($C_{11}H_{17}N_4O$) was used at higher collision energies (40 eV).

A slower gradient from 0 to 60% B over 80 min on a larger column (4.6 mm × 150 mm), eluted at 0.5 ml/min, was used to improve the chromatographic separation for radioactivity detection. The mobile phase was pumped with an Agilent series 1100 pump and the radioactivity was detected by a Radiomatic flo-one beta detector from Packard (CT, USA) equipped with a 0.5 ml flow cell, and 3 ml/min of Ultima FLO was used for scintillation. About 0.05 ml/min of the flow was split after the column to a QuattroLC mass spectrometer from Micromass. The metabolites were detected by electrospray ionisation in the positive ion mode (+ESI) with selected ion recording.

2.4. Deuterium exchange experiments (H_{exch})

The mobile phase water was exchanged with deuterium oxide and the samples were reanalysed by liquid chromatography/mass spectrometry (LC/MS). The mass spectra of the metabolites recorded with water and deuterium oxide were compared and the number of exchangeable protons were calculated from: $H_{\text{exch}} = (M + D) - (M + H) - 1$.

2.5. Nitrogen specific detection

The same stationary phase was used for the LC separation as described above but the internal diameter of the trap and analytical columns were 3 mm. The gradient consisted of buffer A: 2% methanol and 0.02% TFA in water, buffer B: 0.02% TFA in methanol. The sample was eluted at 0.3 ml/min with a gradient from 5 to 50% B during 79 min, 50 to 60% B over 5 min, 60 to 90% B over 5 min continued at 90% B for 4 min. The column effluent was diverted to a chemiluminescent nitrogen detector model 8060 from ANTEK Instruments (Houston, Texas, USA) operated at reactor temperature of 1050 °C and 50 ml/min

of He and 250 ml/min of oxygen. The pressure limit for the nebulizer was set to 11 and 40 psi for low and high, respectively. The photomultiplier was set to 750 V with high amplification.

3. Results

3.1. Mass spectrometric analysis

The product-ion spectrum of protonated BVT.2938 (*m*/*z* 360) recorded at 40 eV collision energy is shown in Fig. 1 together with proposed structures of the registered product-ions. The accurate masses determined are compared with the calculated masses for the proposed structures in Table 1. The proposed structures of the product-ions were generated first by the MassFrontier software from Thermo Finnigan (San Jose, CA, USA) and the results were compared with the determined accurate masses. Thus isobaric product-ions with different elemental composition were differentiated when the mass difference was sufficient. Protonated BVT.2938 appeared to fragment into two isobaric product-ions at *m*/*z* 138.0550 and 138.0667, the first was dominating at low collision energy (10 eV) and the latter at 40 eV. The resolution of the Q-Tof II instrument was insufficient to resolve the isobaric product ions but analysis on another Q-Tof with W reflectron gave higher resolution (10,000) and partial separation of the isobaric product ions. The accuracy of the mass measurements was sufficient to determine the elemental composition of the product-ions as shown in Table 1. The most intense fragment at low collision energy originated from cleavage of the ethylene bridge giving a product-ion at *m*/*z* 221 containing the piperazine and pyrazine ring as shown in Fig. 1.

3.2. Metabolite identification

A scheme of the proposed metabolites of BVT.2938 is shown in Fig. 2. Two radio-chromatograms recorded after incubation of BVT.2938 with human liver microsomes under conditions optimal for CYPs and under conditions optimal for both UGTs and CYPs are compared in Fig. 3A and B, together with a chromatogram recorded after incubation with human hepatocytes (Fig. 3C).

Metabolite M1 had a longer retention time compared to BVT.2938 and its product-ion spectrum (Table 2) showed diagnostic ions at *m*/*z* 237 and 123 suggesting piperazine ring hydroxylation. Since M1 had one exchangeable proton, hydroxylation of the piperazine nitrogen is suggested. The glucuronic acid conjugate of M1, M1GlcA showed diagnostic product ions at *m*/*z* 413 (221 + 16 + 176), 360, 237, and 221. Metabolite M1 was further oxidized to two isomeric nitrones denoted M4. A time course experiment for the formation of M4 metabolites showed that the concentration of the nitrones (M4 metabolites) increased with incubation time from 2.5 to 60 min, but formation of the M1 metabolite decreased at the same time (data not shown). The nitrones had no exchangeable protons and diagnostic product-ions at *m*/*z* 235, 219 and 217. Metabolite M2 consisted of two isomers, which had two exchangeable protons and product-ions at *m*/*z* 221 and 123 indicating pyridine ring hydroxylation. The glucuronides of M2, M2aGlcA and M2bGlcA

Table 1
Comparison of calculated and determined masses for product-ions of BVT.2938

Calculated mass	Collision energy (10 eV)	Collision energy (20 eV)	Collision energy (40 eV)
111.0558, $C_5H_7N_2O$			111.0554 (−0.4)
123.0558, $C_6H_7N_2O$			123.0560 (+0.2)
138.0667, $C_6H_8N_3O$			138.0652 (−1.5)
138.0555, $C_7H_8NO_2$	138.0584 (+2.9)	138.0583 (+2.8)	
152.0824, $C_7H_{10}N_3O$	152.0820 (−0.4)	152.0839 (+1.5)	152.0835 (+1.1)
164.0824, $C_8H_{10}N_3O$		164.0813 (−1.1)	164.0828 (+0.4)
178.0980, $C_9H_{12}N_3O$			178.0982 (+0.2)
191.1297, $C_{10}H_{15}N_4$		+191.1303 (0.6)	
221.1402, $C_{11}H_{17}N_4O$	221.1408 (+0.6)	221.1415 (+1.3)	

The values in parentheses are in millidalton (mDa).

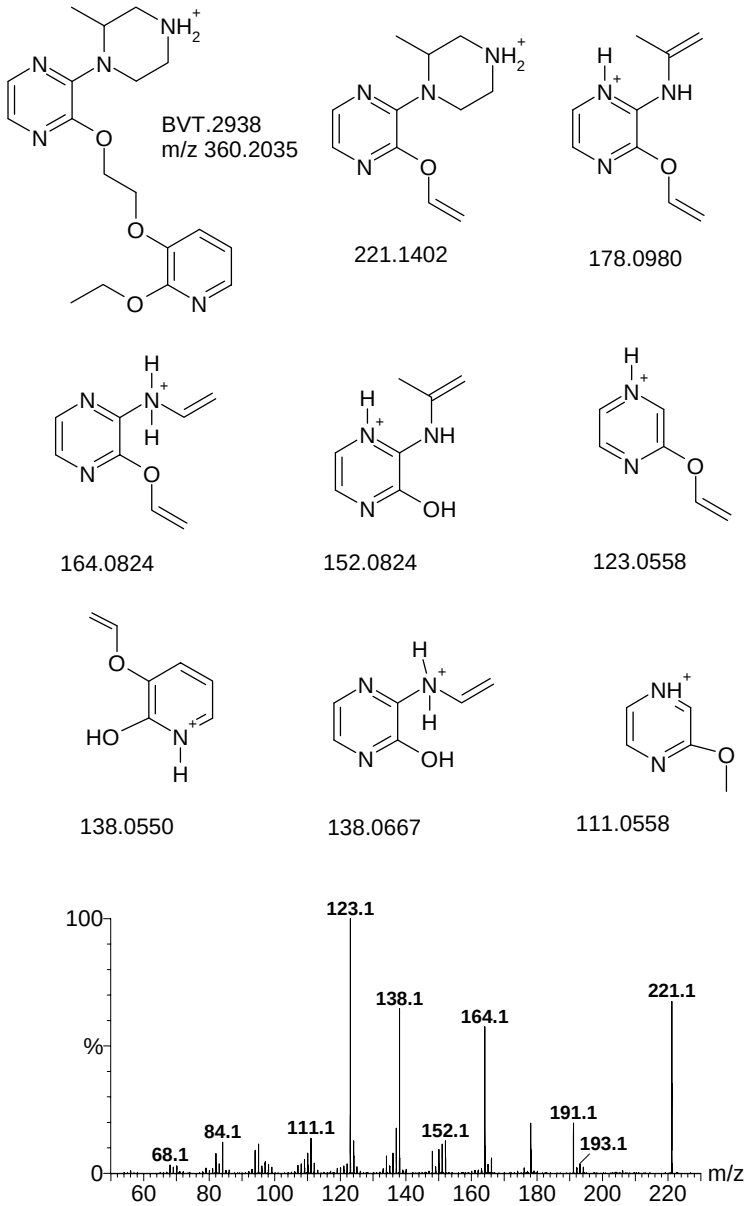

Fig. 1. Product-ion spectrum of BVT.2938 at 40 eV collision energy with Ar as collision gas, together with proposed structures of the product-ions. The product-ion at *m/z* 221 was used for lock mass correction and the determined accurate masses of the other ions are presented in Table 1.

gave an intense product ion at *m/z* 221 and no ion at *m/z* 237 that differed them from the M1 and M3 glucuronides. Metabolite M3 had two exchangeable protons and product-ions at *m/z* 239, 237, 154, 180 indicating pyrazine ring hydroxylation. Analysis of M3 by ^{1}HNMR after preparative fractionation confirmed pyrazine ring hydroxylation but further work is needed to determine if it was hydroxylated at the 5- or 6-position. The glucuronic acid conjugate of M3, M3GlcA gave fragments at *m/z* 376, 239, 237

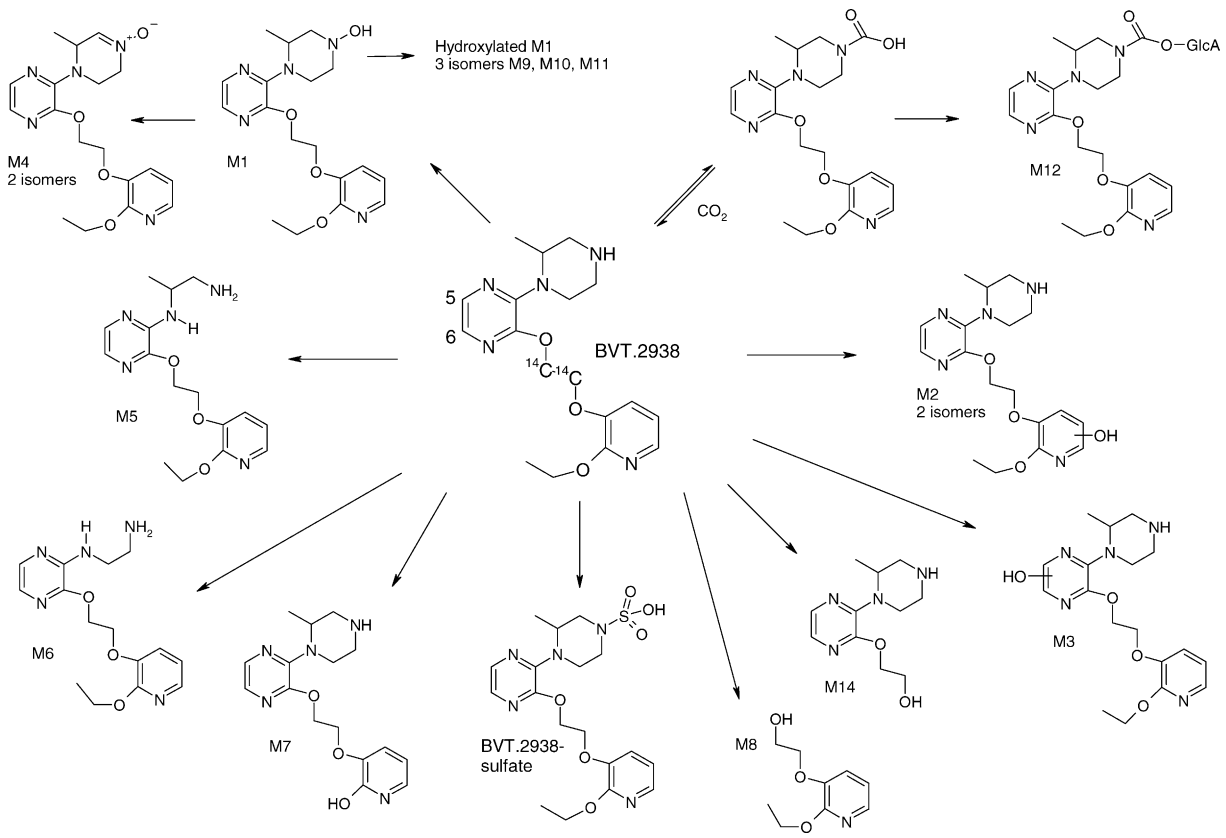

Fig. 2. Tentative identification of BVT.2938 metabolites formed in vitro.

and no fragment at *m/z* 221. Metabolites M5 and M6 had three exchangeable protons and their molecular masses together with the product-ions observed suggested metabolites with an opened piperazine ring as shown in Fig. 2. Metabolite M7 originated from *O*-dealkylation of the ethoxy group of BVT.2938 and M8 from *O*-dealkylation of the ethylene bridge. The product-ion spectrum of M8 was identical to the reference compound BVT.1545. Metabolite M8 was not labelled with ^{18}O during the incubation with $^{18}O_2$ gas and no aldehyde corresponding to M8 was detected in the incubations. All other metabolites formed after hydroxylation incorporated the ^{18}O label to about 98% during incubation with $^{18}O_2$. Metabolites M9, M10 and M11 had two exchangeable protons and originated from hydroxylation of M1 at the pyrazine and pyridine rings. The product-ion spectrum of metabolite M12 showed a characteristic loss of 176 Da to *m/z* 404 indicating that it was a glucuronic acid conjugate (Fig. 4). The fragment at *m/z* 404 lost 44 Da (CO_2) to give *m/z* 360 (protonated BVT.2938) which suggested that M12 was a carbamoyl-glucuronide. Attempts were made to produce the carbamate of BVT.2938 by reaction with 1 M ammonium hydrogen carbonate. The solution was diluted to 20 mM hydrogen carbonate and infused into the mass spectrometer. The base peak in the spectrum corresponded to protonated BVT.2938 but a peak at *m/z* 404 (5%) was also observed. The product-ion spectrum of *m/z* 404 (Table 2) suggested that it was the carbamate of BVT.2938 either formed in solution or in the gas-phase during ionization in the mass spectrometer. Attempts to separate the BVT.2938-carbamate from BVT.2938 by reversed-phase chromatography with ammonium hydrogen carbonate as buffer were not successful. Metabolites M5, M6, M8 and M14

Table 2
Molecular mass, number of exchangeable protons and product ions of BVT.2938 and its metabolites

Metabolite	*m/z*	H_{exch}	Product ions above 5% relative abundance at 10, 20 or 40 eV collision energy
Parent	360	1	221, 191, 178, 164, 152, 138, 123, 111
M1	376	1	237, 219, 192, 191, 177, 164, 150, 138, 123, 111, 96
M1GlcA[a]	552	N.M.[b]	413, 360, 358, 277, 237, 221, 192, 166, 138
M2	376	2	221, 191, 178, 164, 154, 138, 123, 111
M2aGlcA	552	N.M.	376, 221, 164, 154, 123
M2bGlcA	552	N.M.	376, 221, 182, 166, 154, 138
M3	376	2	239, 237, 182, 180, 154, 140, 138, 126, 112, 94, 83
M3GlcA	552	N.M.	376, 239, 237, 182, 154, 140, 138, 112
M4	374	0	357, 356, 235, 219, 217, 191, 173, 162, 150, 148, 138, 119, 94, 80
M5	334	3	195, 180, 178, 152, 138, 110, 94
M6	320	3	181, 166, 164, 152, 138, 111
M7	332	2	221, 195, 152, 138, 111, 94
M8	184	1	156, 138, 112, 94, 82, 67, 66
M9	392	2	253, 182, 140, 138, 112
M10	392	2	237, 150, 138, 123
M11	292	2	374, 237, 166, 154, 138
M12	580	N.M	441, 404, 360, 265, 221, 138
M13	364	1	318, 221, 219
^{18}O-M13	368		320, 221, 219
M14	239	2	196, 182, 152, 138, 111, 93, 83, 83, 79
BVT.2938-carbamate	404	N.M	360, 265, 221, 191, 178, 164, 138, 123, 111
BVT.2938-sulfate	440	1	360, 223, 221, 191, 178, 164, 138, 123

[a] GlcA: glucuronic acid conjugate.
[b] N.M.: not measured.

were not conjugated as fast as M1, M2 and M3 and their glucuronides were below the detection limit by LC/MS. BVT.2938-sulphate had one exchangeable proton and showed a characteristic loss of 80 Da which suggested that the piperazine nitrogen had been conjugated with sulphuric acid.

Metabolite M13 was measured to 364.1985 Da, which suggests an elemental composition of $C_{17}H_{26}N_5O_4$, that is a carbon atom less, and an oxygen atom more compared to the parent compound. BVT.2938 was incubated with recombinant expressed CYP2D6 in an atmosphere of $^{18}O_2$ to check if ^{18}O was incorporated in the metabolite by cytochrome P450. The product-ion spectra of this metabolite and the ^{18}O-labelled metabolite are shown in Table 2. The spectra in Table 2 suggest that the pyridine ring had been altered but this was not investigated further since it was a minor metabolite. Metabolite M14 was detected at *m/z* 239 and its product-ion spectrum in Table 2 suggested that this was another metabolite originating from *O*-dealkylation of the ethylene bridge of BVT.2938 with the same mechanism as M8 since M14 was not labelled during incubation with $^{18}O_2$.

3.3. Metabolite separation and quantification

All metabolites were well separated in ion-current chromatograms from LC/MS but it was difficult to separate all metabolites with radioactivity detection for quantification. Peak numbers 8 and 9 in Fig. 3B consisted of M8 + M2a and M5 + M2b, respectively. When UDPGA was added to the incubation M2 was conjugated with glucuronic acid to about 90% as detected by LC/MS and peaks 8 and 9 in Fig. 3A were much less interfered with by the M2 isomers. Thus when the relative peak areas in Table 3 are compared one can conclude that *O*-dealkylations to M7 and M8, hydroxylation of pyridine ring (M2) and pyrazine ring (M3) together with piperazine ring scission (M5) were the major metabolites in human hepatocytes. Direct conjugation with sulphuric acid was important in hepatocytes and the carbamoyl-glucuronide of BVT.2938 (2.2%) was detected in human microsomes

Table 3
Relative metabolite peak area of radio-chromatograms after incubation of labelled BVT.2938 with liver microsomes and cryopreserved hepatocytes from man, monkey and rat

Peak no./ T_R (min)	Metabolite	HLM[a]	HLM + UDPGA	HH[b]	MLM[c]	MLM + UDPGA	MH[d]	RLM[e]	RLM + UDPGA	RH[f]
1/16.5	M14	1.3	0.4	N.D.	4.3	N.D.	N.D.	7.1	0.7	N.D.
2/21.3	M3GlcA	N.D[g]	1.2	1.4	N.D.	8.1	17	N.D.	21.3	7.7
3/23.3	M7	6.1	2.4	4.8	4.2	4.9	4.5	7.9	5.4	6.2
4/28.1	M2GlcA	N.D.	0.8	2.7	N.D.	2.2	5.6	N.D.	6.1	14
5/28.7	M3	6.6	3.3	0.3	32	14	8.6	12	6.1	N.D.
6/29.3	M2GlcA	N.D.	4.6	8.5	N.D.	9.0	2.8	N.D	3.7	1.8
7/30.3	M6	0.9	0.6	N.D.	N.D.	1.3	N.D.	1.2	0.8	0.9
8/31.1	M8 + M2a	15	9.6	5.1	42	37	29	26	16	11
9/32.3	M5 + M2b	17	5.2	1.0	4.6	4.8	2.5	15	18	N.D.
10/34.4	BVT.2938	49	63	70	0.7	6.1	23	3.7	3.3	41
11/39.2	M1	3	1.4	N.D.	0.3	0.4	N.D.	2.3	N.D.	2.0
12/43.1	M4	1.1	1.1	0.5	1.8	2.1	N.D.	18	21	3.0
13/44.9	M4 + M1GlcA	0.4	3.8	2.1	1	2	0.9	4.4	10	5.6
14/46.0	M12	N.D.	2.2	N.D.	N.D.	5.2	N.D.	N.D.	1.4	N.D.
15/50	BVT.2938-sulfate	N.D.	N.D.	4.6	N.D.	N.D.	1.8	N.D.	N.D.	1.4

[a] Human liver microsomes.
[b] Human hepatocytes.
[c] Monkey liver microsomes.
[d] Monkey hepatocytes.
[e] Rat liver microsomes.
[f] Rat hepatocytes.
[g] Not detected.

supplemented with UDPGA. *O*-dealkylation to M8, pyrazine ring hydroxylation to M3 and glucuronidation via carbamate were the major metabolites in the monkey. The rat produced more of the *O*-dealkylation product M14 and the nitrone metabolites M4 compared with man and the monkey. An extended gradient with methanol as modifier instead of acetonitrile separated most of the rat metabolites as shown in Fig. 5. The relative peak areas obtained from CLND, radioactivity and MS (SIR) for the same rat microsomal sample are shown in Table 4.

4. Discussion

Quadrupole-time of flight mass spectrometry offers new possibilities for structural analysis of drug metabolites since accurate mass determinations of

Table 4
Comparison of relative peak area response from CLND, radioactive and MS detection of BVT.2938 metabolites from rat liver microsomes

Metabolite	Peak no.	N atoms	CLND corrected for N	Radioactivity detection	MS (SIR)
M14	1	4	6.2	5.6	2.6
M7	2	5	9.7	10.3	5.4
M8	3	1	29.2	30.7	46.5
M3a + M3b	4	5	5.8	5.7	3.7
M2a	5	5	5.7	5.7	2.5
M2b	6	5	5.6	5.0	3.3
M5	7	5	13.6	13.4	16.1
BVT.2938	8	5	7.3	8.1	7.7
M4a	9	5	9.8	9.0	8.0
M4b	10	5	7.1	6.5	4.1

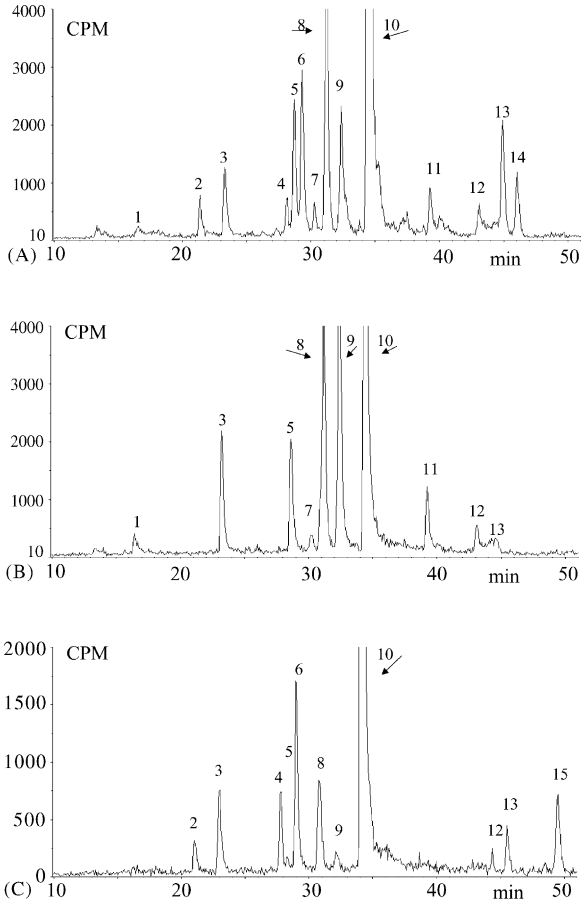

Fig. 3. Comparison of radio-chromatograms from human liver microsomes supplemented with NADPH and UDPGA (A), human liver microsomes with NADPH but without UDPGA (B) and human cryopreserved hepatocytes (C). The metabolites were separated with an acetonitrile gradient (2–60%) over 80 min on a Luna C18 column (4.6 mm × 150 mm). 1 (M14), 2 (M3GlcA), 3 (M7), 4 (M2aGlcA), 5 (M3), 6 (M2bGlcA), 7 (M6), 8 (M8 + M2a), 9 (M5 + M2b), 10 (BVT.2938), 11 (M1), 12 (M4a), 13 (M4b + M1GlcA), 14 (M12) and 15 (BVT.2938-sulfate).

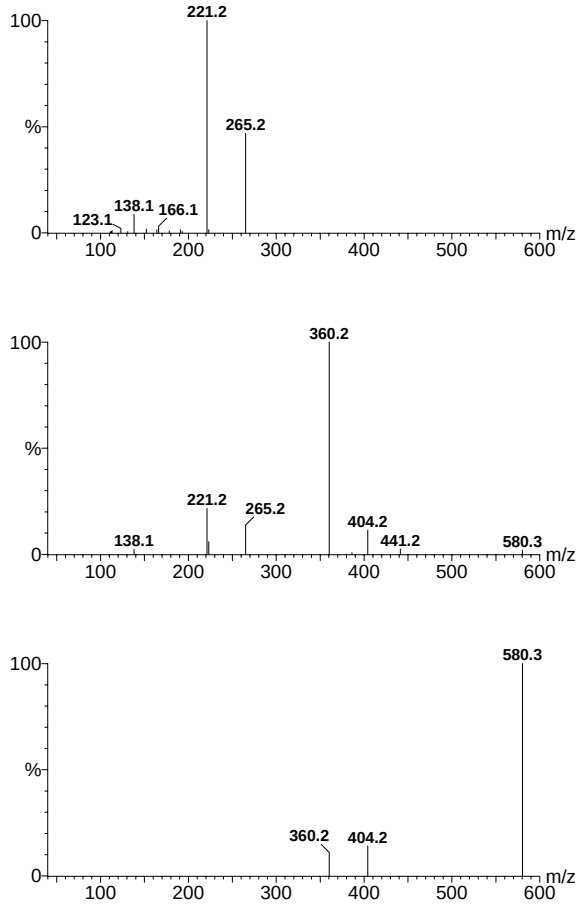

Fig. 4. Product-ion spectrum of protonated M12, the carbamoyl-glucuronide of BVT.2938 (*m*/*z* 580) showing losses of GlcA to *m*/*z* 404 and further loss of CO_2 to *m*/*z* 360. Additional fragments are shown at *m*/*z* 441 from the piperazine and pyrazine rings plus carbamoyl-glucuronide (221 + 176 + 44 Da) and at 265 Da (221 + 44 Da). The product-ion spectra were recorded at collision energies of 10 eV (bottom), 20 eV (middle) and 40 eV at the top. The accumulation time was 1 s for each collision-energy.

both precursor and product-ions can be obtained with high sensitivity, which improves the certainty of the proposed fragmentation pathways [6]. The mass differences between the calculated and determined masses of the product-ions of BVT.2938 were less than 2 mDa (Table 2), which was sufficient to define their elemental composition, since the elemental composition of the precursor-ion could be used as an upper limit. Additional structural information can be obtained by deuterium exchange [1,3]. This approach was very useful to differentiate between carbon and nitrogen hydroxylation at the piperazine ring of BVT.2938. It was also useful to confirm the nitrones of the piperazine ring, which had no exchangeable protons. Previously, several primary and secondary amine-containing drugs including tocainide [7], rimantadine [8], mofegiline [9], carvedilol [10] and sertraline [11] have been shown to be converted to carbamoyl-glucuronide conjugates in vivo. The formation of a carbamoyl-glucuronide

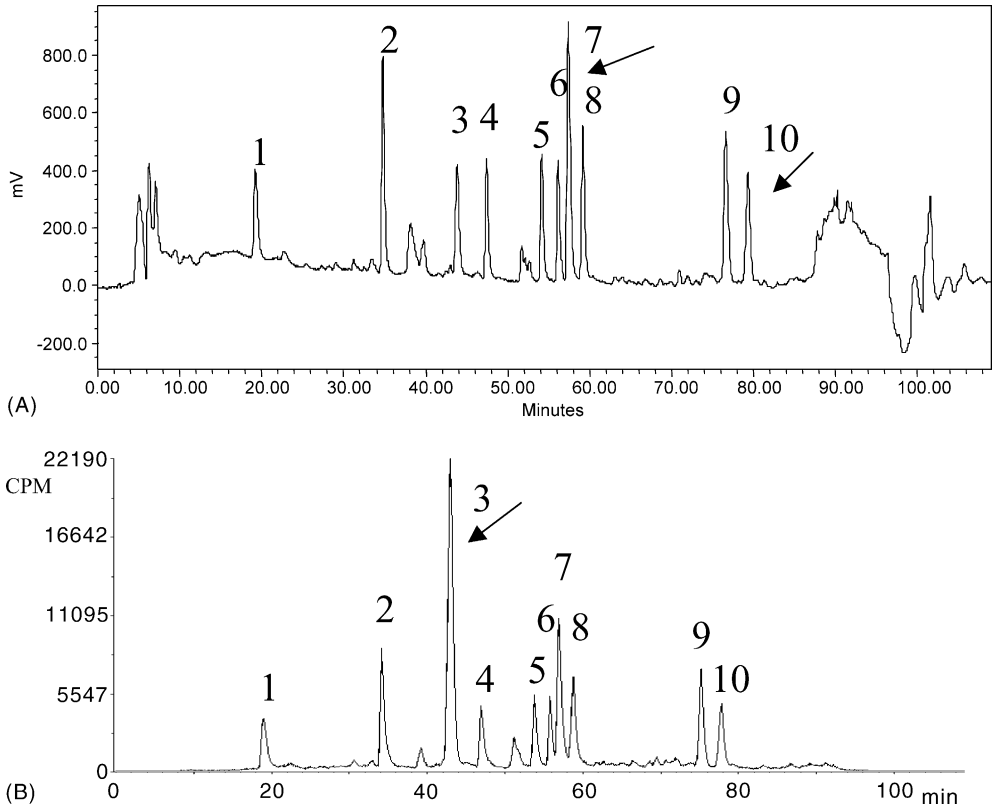

Fig. 5. Comparison of LC-CLND chromatogram (A) and radioactivity chromatogram (B) obtained after injection of 0.3 ml sample from incubation of labelled BVT.2938 with rat liver microsomes. The sample was separated on a 3 mm × 150 mm column packed with 5 μm Luna C18 particles and eluted at 0.3 ml/min with a gradient from 5 to 50% B over 79 min, 50 to 60% B during 5 min, 60 to 90% B during 5 min continued at 90% B for 4 min 1 (M14), 2 (M7), 3 (M8), 4 (M3a + M3b), 5 (M2a), 6 (M2b), 7 (M5), 8 (BVT.2938), 9 (M4a) and 10 (M4b).

of carvedilol in vitro using liver microsomes has also been demonstrated [10]. The metabolites are probably formed by the chemical reaction of the amine with carbon dioxide followed by enzymatic glucuronidation of the carbamate forming a stable conjugate. The parent compound is recovered after enzymatic or acidic hydrolysis due to the reversibility of the carbamate formation. Thus a soft ionisation technique like electrospray ionisation is required to determine the molecular mass of the conjugates and enzymatic hydrolysis alone will not identify carbamoyl-glucuronides. The carbamoyl-glucuronide of BVT.2938 was not expected but the sulphate and carbamoyl-glucuronide of BVT.2938 were detected in urine of animals after the first in vivo studies. To our knowledge carbamoyl-glucuronides of piperazines have not been reported earlier. This type of conjugation could be of importance for the metabolic clearance of BVT.2938 in vivo and this pathway would not be detected at conventional conditions for in vitro incubations using liver microsomes. Therefore, in this study we used incubation conditions for simultaneous activation of both CYP and UGT activities including a source of carbon dioxide for formation of carbamoyl-glucuronide [10,12]. Under such conditions we were able to identify not only the carbamoyl-glucuronide of BVT.2938 but also glucuronides of phase I metabolites. The product-ion spectrum of the protonated carbamoyl-glucuronide of BVT.2938 was sufficient for a tentative identification of this metabolite, since characteristic losses of 176 Da (GlcA) and 176 + 44 Da (GlcA + CO_2) were detected and these losses are diagnostic for carbamoyl-glucuronides [7–11]. Ethanolysis of the

carbamoyl-glucuronide of carvedilol to form ethyl carbamate have been described to confirm the identity of this metabolite [10].

Piperazine *N*-oxidation has been described [13] and it has been proposed that the hydroxylamine metabolite of *N*-deacetyl ketoconazole could be oxidized to a nitrone by flavine containing monooxygenases [14]. A time course experiment for metabolite formation of BVT.2938 supported the hypothesis that M4 was formed from M1. Ethylenediamine metabolites of ketoconazole have also been reported and probably formed via 2,3-piperazinedione or piperazinediol. However, we did neither detect any formation of piperazinediones or diols of BVT.2938 nor did we detect any further reaction products of the piperazine-ring opened metabolites M5 and M6. Hydroxylation at the aromatic rings and the *O*-dealkylation reactions at the ethylene bridge and deethylation of the pyridine ring were all expected but the mechanism for formation of M8 and M14 by *ipso*-substitution of the oxygen at the aromatic rings were not expected. The pyrazine dealkylation product was not detected since it did not carry the ^{14}C-label and went undetected by MS. *O*-dealkylation of ethers usually occurs by α-carbon oxidation followed by hydroxylation and hydrolysis to phenol (or alcohol) plus a carbonyl compound [15]. The *ipso*-substitution of aromatic oxygen has been demonstrated for other arylethers [16,17] and would be undetected unless ^{18}O labelling experiments are performed. To determine the position of the hydroxyl group in metabolites M2 and M3 will require analysis by NMR and synthesis of the metabolites, which will be performed on a later stage if required.

The metabolite patterns after incubation with hepatocytes, were similar to microsomes with activated CYPs and UGTs with two exceptions. BVT.2938-sulphate was identified as an additional metabolite of BVT.2938 in hepatocyte incubations. Nevertheless, the carbamoyl-glucuronide was not present in these incubations. The absence of the carbamoyl-glucuronide in the hepatocyte incubations and the presence in microsomal incubations was most probably due to differences in hydrogen carbonate buffer concentration between these two systems. Thus it seems difficult to generate all possible metabolites in a single in vitro experiment. For metabolite identification from in vitro experiments on primary and secondary amines we propose that two different incubation conditions are used, with CYP activation and CYP + UGT activation. Since the enzyme activity is high in microsomes sufficient of metabolites is produced to obtain mass spectra of good quality for structural analysis. Incubations with hepatocytes or liver slices can be used in order to cover metabolism by non-microsomal enzymes, i.e. sulphotransferases and glutathione *S*-transferases.

This strategy identified three different metabolic reactions of the secondary amine group of the piperazine-ring of BVT.2938: hydroxylation to hydroxylamine, carbamate formation followed by glucuronidation to carbamoyl-glucuronide and N-sulphoconjugation. To estimate the contribution of these metabolites to the biotransfomation of BVT.2938 and to identify the enzymes responsible for the formation of the metabolites, additional enzyme kinetic studies have been initiated. However, the full importance and understanding of the sulphation and carbamoyl glucuronidation pathway for metabolism of BVT.2938 can only be answered after in vivo administration of labelled drug to animals and humans. An attractive alternative on an early stage in drug development could be to generate metabolites in vitro and quantify them by chemiluminescent nitrogen detection to establish a standard solution as shown in Fig. 5 and Table 4. Provided that the metabolites can be separated from each other and nitrogen containing matrix components, such a standard solution can then be used to optimise selection of product ions, collision energies and declustering potentials for quantification of metabolites in plasma and urine by LC/MS/MS. The standard can be used for calibration and quantification with sufficient accuracy to determine if the metabolites are major or minor metabolites in animals and humans. The detection limit of the CLND was 20 pmol N and the background from liver microsome extracts was low. The detector was less useful for quantification of metabolites in urine due to interference from numerous matrix components containing nitrogen.

Acknowledgements

The authors would like to thank Dr. Hans Postlind for support and helpful discussions. Anders Dyremark and Åse Husman-Sjöblom for technical assistance.

References

[1] P.O. Edlund, J. Mass Spectrom. 30 (1995) 1380–1392.
[2] D.Q. Liu, C.E.C.A. Hop, M.G. Beconi, A. Mao, S.A. Lee Chiu, Rapid Commun. Mass Spectrom. 15 (2001) 1832–1839.
[3] N. Ohashi, S. Furuuchi, M. Yoshikawa, J. Pharm. Biomed. Anal. 18 (1998) 325–334.
[4] E.W. Taylor, M.G. Qian, G.D. Dollinger, Anal. Chem. 74 (2002) 3232–3238.
[5] E.W. Taylor, W. Jia, M. Bush, G.D. Dollinger, Anal. Chem. 70 (1998) 3339–3347.
[6] G. Hopfgartner, F. Vilbois, Analusis 28 (2000) 906–914.
[7] D.W.K. Kwok, G. Pillay, R. Vaughan, J.E. Axelson, K.M. McErlane, J. Pharm. Sci. 79 (1990) 857–861.
[8] S.Y. Brown, W.A. Garland, E.K. Fukuda, Drug. Metabol. Dispos. 18 (1990) 546–547.
[9] J. Dow, F. Piriou, E. wolf, B.D. Dulery, K.D. Haegle, Drug. Metabol. Dispos. 22 (1994) 738–749.
[10] W.H. Schaefer, Drug. Metabol. Dispos. 20 (1992) 130–133.
[11] L.M. Tremaine, J.G. Stroh, R.A. Ronfeld, Drug. Metabol. Dispos. 17 (1989) 58–63.
[12] M.B. Fisher, K. Campanale, B.L. Ackermann, M. Van den Branden, S.A. Wrighton, Drug Metabol. Dispos. 28 (2000) 560–566.
[13] D. Luffer-Atlas, S.H. Vincent, S.K. Painter, B.H. Arison, R.H. Stearns, S.H. Lee Chiu, Drug Metabol. Dispos. 25 (1997) 940–952.
[14] R.J. Rodriguez, P.J. Proteau, B.L. Marquez, C.L. Hetherington, C.L. Buckholz, K.L. O'Connel, Drug Metabol. Dispos. 27 (1999) 880–886.
[15] B. Testa, Biochemistry of Redox Reactions, Academic Press, London, 1995, pp. 236–240.
[16] T. Ohe, T. Mashino, M. Hirobe, Arch. Biochem. Biophys. 310 (1994) 402–409.
[17] T. Ohe, T. Mashino, M. Hirobe, Tetrahedron Lett. 42 (1995) 7681–7684.